

Anomalous Loss Behavior in a Single-Component Fermi Gas Close to a p -Wave Feshbach Resonance

K. Welz,¹ M. Gerken,¹ B. Zhu,² E. Lippi,¹ M. Rautenberg,¹ L. Chomaz,^{1,*} and M. Weidemüller^{1,†}

¹*Physikalisches Institut, Universität Heidelberg, Im Neuenheimer Feld 226, 69120, Heidelberg, Germany*

²*HSBC Lab-China, Guangzhou 510620, China*

(Dated: October 31, 2022)

We theoretically investigate three-body losses in a single-component Fermi gas near a p -wave Feshbach resonance in the interacting, non-unitary regime. We extend the cascade model introduced by Waseem *et al.* [Phys. Rev. A **99** 052704 (2019)] to describe the elastic and inelastic collision processes. We find that the loss behavior exhibits a n^3 and an anomalous n^2 dependence for a ratio of elastic to inelastic collision rate larger and smaller than one, respectively. The corresponding evolutions of the energy distribution show collisional cooling or evolution toward low-energetic non-thermalized steady states, respectively. These findings are in particular relevant for understanding atom loss and energetic evolution of ultracold gases of fermionic lithium atoms in their ground state.

I. INTRODUCTION

Magnetic Feshbach resonances are essential for tuning the collisional properties of ultracold atomic and molecular gases [1, 2]. The minimal model of Feshbach resonances takes into account two coupled collision channels, the scattering channel and a closed channel with a bound state whose energy lies, and can be tuned around, the scattering threshold of the open channel. Together with the resonant behavior of the elastic binary collisions, also inelastic collisions are altered near magnetic Feshbach resonances. Understanding inelastic collisions and the related losses near such resonances has been essential for their exploitation. As a paradigmatic example, the stability of a degenerate two-spin Fermi sample, caused by the suppression of possible loss processes [3, 4], led first to the production of a Bose-Einstein condensate of Fermi dimers [5] and later to the investigation of the BEC-BCS crossover [6–8].

In the ultracold regime, collisions in the s -partial wave typically dominate, see e.g. [1, 2]. However, in the case of fermions, s -wave collisions are precluded between identical particles. Feshbach resonances enhancing the p -wave scattering (so called p -wave Feshbach resonances) have been observed [9, 10] between fermions of the same spin state. Interest in resonantly p -wave interacting fermions arises in particular from the possibility of a rich quantum phase diagram involving anisotropic p -wave superfluidity [11, 12]. Such phases, however, require particularly low temperatures. Driven by this interest, great theoretical and experimental effort has been devoted to understand the elastic and inelastic scattering processes close to p -wave Feshbach resonances [9, 10, 13–16]. For the case of two-component Fermi gases with resonant s -wave interactions, inelastic processes of two-body nature, induced by dipole-dipole interactions, domi-

nate [10, 17]. A single-component Fermi gas prepared in the lowest hyperfine state suppresses spin-flip relaxation such that the dominant inelastic process should involve three atoms [9, 10, 15, 16, 18].

One possibility for the scattering of three p -wave interacting fermions is the direct collision of three atoms leading to their recombination into a deeply-bound dimer and one atom, with a large amount of energy released [18]. However, as mentioned above, this effect is strongly suppressed due to Fermi statistics and instead, in some regimes, it was hypothesised that the dominant process for the scattering of three atoms involves an intermediate stage, in which a weakly-bound dimer is created before colliding with a third atom. To describe losses in the latter regime and explain experimental observations in ground-state ^6Li atoms in the vicinity of a p -wave Feshbach resonance, Waseem *et al.* used a cascade model in which the inelastic process is split into two steps [19], see also [20]. First, two atoms form a weakly-bound dimer via elastic scattering. Second, the dimer is vibrationally quenched to a deeply bound state by inelastic collision with an observer atom, resulting in the loss of the three atoms. Alternatively, the weakly bound dimer can break up into two free atoms, leading to an overall elastic scattering event.

In this paper we present an extension of the cascade model studied in Waseem *et al.* [19] by investigating the two extreme regimes of the ratio of the rates of elastic-to-inelastic collisions. In the first regime where elastic collisions dominate over inelastic collisions, we find as in ref. [19] that the atom-loss behavior remains that of a three-body process. Furthermore, we investigate the temperature and phase-space density evolution and we identify the regimes of collisional heating and collisional cooling as a function of the ratio of the dimer binding energy to the mean thermal energy. The possibility of collisional cooling is similar to earlier findings, see e.g. [21–25]. In the second regime where inelastic collisions dominate, we find that the loss

* chomaz@physi.uni-heidelberg.de

† weidemuller@uni-heidelberg.de

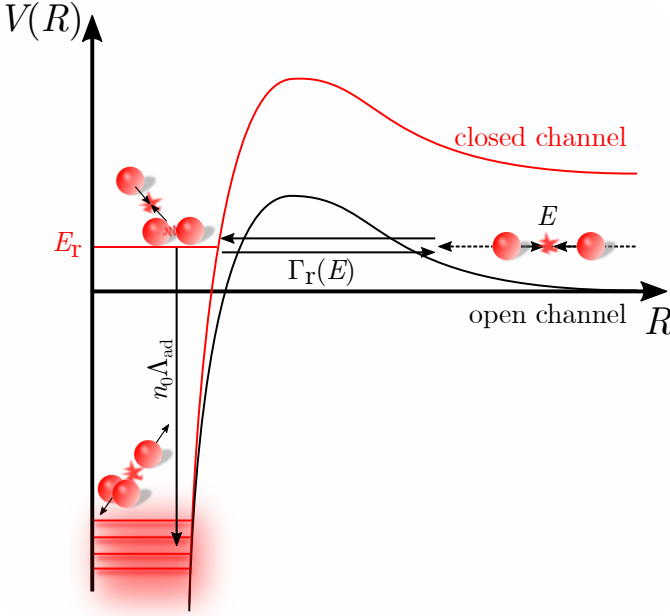


FIG. 1. Schematic depiction of the p -wave scattering process. The figure shows the potential of the incoming scattering atoms at energy E and the closed channel with a resonant dimer state at energy E_r . Incoming atoms can tunnel through the centrifugal barrier and create weakly-bound dimers with a rate coefficient L_M . Weakly-bound dimers can, in return, decay into two free atoms with rate $\Gamma_r(E)$. This elastic scattering process leads to energy redistribution e.g. thermalization. Weakly-bound dimers colliding with a free atom leads to collapse into a deeply-bound dimer at rate $n_0\Lambda_{ad}$, with n_0 the initial density of the atoms. This inelastic process leads to a loss since the binding energy sets free kinetic energy large compared to the trap depth of the atomic trap.

dynamic distinctly follows that of an effective two-body process. Due to the slow thermalization compared to the losses, and due to the energy dependence of the collision processes, the momentum distribution is found to evolve to a low-energy non-thermal steady state.

The paper is organised as follows. In section II, we describe the elastic and inelastic collisions via a cascade model and explain the basic assumptions needed for the model and for separating the two loss behaviour regimes. Atom loss and temperature evolution in the thermalized regime are described in section III A. The non-thermalized regime with an expansion to an energy-dependent model of the losses is studied in III B. We conclude in section IV.

II. COLLISIONAL CASCADE MODEL

In our model, we consider free identical fermions colliding in a p -wave open channel and a unique weakly-bound dimer state of energy E_r in a closed channel that induces a resonant behavior of the scattering, see FIG. 1. The

elastic and inelastic collisions are each described by a cascade of two processes, as in ref. [19]. Both cascades start with the formation of a weakly-bound dimer in the collision of two free atoms. In the elastic collision case, the second process is the break-up of this dimer back into two free atoms, see solid arrow pointing to the right in FIG. 1. Here, a redistribution of kinetic energy between the colliding atoms can occur.

In the inelastic collision case, instead, the second process is the collision of the weakly-bound dimer with a free atom and its relaxation into a deeply-bound dimer, see vertical arrow in FIG. 1. In the latter process, a third atom is necessary because of energy and momentum conservation. With the relaxation to the deeply-bound state, both the atom and dimer acquire large kinetic energy such that they leave the trap and are irreversibly removed from the system of interest. As a consequence, the relaxation is an irreversible process in contrast to the creation and break-up of the weakly-bound dimer.

The inelastic and elastic cascades compete and their dynamic can be described with two coupled differential equations describing the evolution of the density of free atoms, n , and that of weakly-bound dimers, n_D [19, 20]:

$$\frac{dn_D}{dt} = +L_M n^2 - \Gamma_r n_D - \Lambda_{ad} n n_D \quad (1)$$

$$\frac{dn}{dt} = -2L_M n^2 + 2\Gamma_r n_D - \Lambda_{ad} n n_D \quad (2)$$

For both equations, the first term describes the creation of a weakly-bound dimer from two free atoms with rate coefficient L_M . The second term corresponds to the break-up of a weakly-bound dimer with rate Γ_r . The last term describes the atom-dimer collision with rate coefficient Λ_{ad} , yielding losses from the system. These equations neglect other loss processes such as the collision with background gases, dimer-dimer relaxation, and direct three-body recombination, which are assumed to be slow compared to the investigated processes.

We now aim to relate the rate coefficients relevant for the cascade model to the parameters describing the scattering close to a p -wave resonance. We first consider the general case of two atoms of mass m and velocities \vec{v} and \vec{v}' . Their relative collisional energy is given by $E = m|\vec{v} - \vec{v}'|^2/4 = mv_{rel}^2/4 = \hbar^2 k^2/m$. The p -wave scattering phase shift $\delta_p(k)$ can be described by an effective range expansion: $k^3 \cot(\delta_p(k)) = -V_p^{-1} - k_e k^2$, where V_p is the scattering volume and k_e is the effective range of the potential [26]. The p -wave scattering amplitude is then given by $f_p(k) = k^2/[k^3 \cot(\delta_p(k)) - ik^3]$, in the limit of $|V_p|^{-1} \ll k_e^3$, and diverges for the energy:

$$E_{pole} = \frac{\hbar^2}{m|V_p|k_e} - i \frac{2\sqrt{m}E^{3/2}}{k_e \hbar} \quad (3)$$

From the real part of Eq. (3) we deduce that the molecular bound state exists at the resonance position $E_r =$

$\hbar^2/(m|V_p|k_e) = \hbar^2 k_r^2/m$ for $V_p < 0$. From the imaginary part of Eq. (3) we infer that its energy-dependent break-up rate in two free atoms of relative energy E , is given by $\Gamma_r(E) = 2\sqrt{m}E^{3/2}/(k_e\hbar^2)$ [27]. It is interesting to note that $\hbar\Gamma_r(E_r) = 2E_r/\sqrt{|V_p|k_e^3} \ll E_r$ holds in the limit considered above. The energy-dependent rate coefficient at which two atoms of relative collisional energy E form a weakly bound dimer is given by [21]

$$K_M(E) = v_{\text{rel}} \frac{\pi}{k^2} \frac{3\hbar^2\Gamma_r(E)^2}{(E - E_r)^2 + \hbar^2\Gamma_r(E)^2/4} \quad (4)$$

and depends on the resonance width $\Gamma_r(E)$ and the resonance energy E_r .

In this paper, we focus on the regime where the cascade model explains the dominant loss process, in contrast to the non-interacting regime and the unitary regime, where direct three-body recombination dominates over the cascade effect, see appendix A. This regime corresponds to $3k_B T/2 \sim E_r$ and distinguishes itself from the unitary (non-interacting) regime via $3k_B T/2 > E_r$ ($3k_B T/2 < E_r/10$) [15, 19] where T is the gas temperature and k_B is the Boltzmann constant. In the interacting non-unitary regime of interest, we can thus assume $\hbar\Gamma_r(E_r) \ll k_B T$ (limit of $|V_p|^{-1} \ll k_e^3$). In this case, one can approximate the dimer formation rate coefficient by a Dirac delta distribution, $K_M(E) \approx \Gamma_r(E_r) \frac{3}{2\pi} \left(\frac{2\pi}{k_r}\right)^3 \delta(1 - E/E_r)$. This implies that two colliding atoms must have a relative energy matching E_r to be able to form a dimer. As a consequence, we can approximate the collision rates as energy independent as done in Eqs. (1)-(2) with the dimer break-up rate given by $\Gamma_r(E_r) = \Gamma_r$, and the dimer creation rate coefficient defined by a thermal averaging of $K_M(E)$, $L_M = 3\Gamma_r(6\pi/k_T^2)^{3/2} e^{-E_r/(k_B T)}$, with $k_T = \sqrt{3mk_B T/2}/\hbar$ the thermal wavenumber. The rate coefficient Λ_{ad} , quantifying the atom-dimer collision rate, is taken to be constant and independent of the dimer's and atom's momenta.

To describe the losses of atoms, we apply a final assumption as in ref. [19]: We assume that the density of weakly-bound dimers, which is an intermediate product in the processes, is always in a steady state on the timescale of the atom losses, see the sign difference in the terms of Eqs. (1)-(2). Therefore we use $\frac{dn_D}{dt} = 0$ and find $n_D = L_M n^2/(n\Lambda_{\text{ad}} + \Gamma_r)$. The density-loss equation can then be rewritten as:

$$\frac{dn}{dt} = -\frac{9\Lambda_{\text{ad}}\Gamma_r}{n\Lambda_{\text{ad}} + \Gamma_r} \left(\frac{6\pi}{k_T^2}\right)^{3/2} e^{-E_r/(k_B T)} n^3 \quad (5)$$

In appendix A, we extract the scattering and loss parameters for a p -wave Feshbach resonance (close to $B = 160$ G) of ^6Li in the spin state $|F, m_F\rangle = |1/2, 1/2\rangle$ using the measurements of Ref. [19]. We demonstrate that the interacting non-unitary regime can be reached

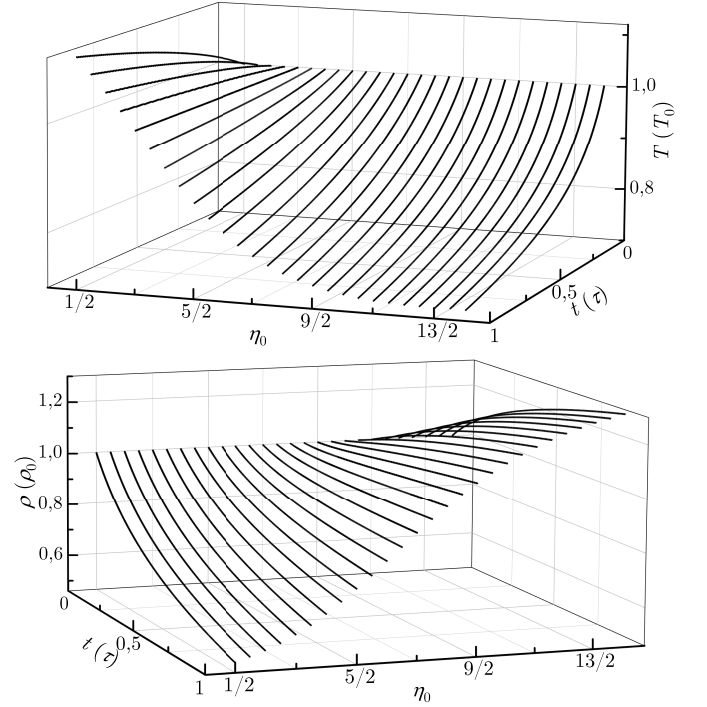


FIG. 2. The temperature T in units of the initial temperature $T_0 = T(t=0)$ (upper panel) and the phase-space density ρ in units of $\rho_0 = \rho(t=0)$ (lower panel) of a gas in the thermal regime for different truncation parameters η_0 after a hold time t in units of τ in a box potential. The temperature decreases for $\eta_0 > 3/2$ and the phase-space density increases for $\eta_0 > 9/2$.

experimentally while still being able to change the ratio $\Gamma_r/(n_0\Lambda_{\text{ad}})$.

In the following, we investigate the consequences of Eq. (5) in two limiting scenarios leading to the separation of a thermalized and a non-thermalized regime.

III. RESULTS

A. Thermalized Regime

We start by investigating the regime where (A) $\Gamma_r \gg n\Lambda_{\text{ad}}$. That is the creation and break-up of weakly-bound dimers happening fast compared to the relaxation into a deeply-bound dimer. Considering the two scattering outcomes, this condition implies a large elastic to inelastic collision ratio, and therefore a thermalized regime.

In this thermalized regime, Eq. (5) simplifies to

$$\frac{dn}{dt} = -L_3 n^3. \quad (6)$$

with the inelastic scattering process yielding an effective three-body decay of the density with the three-body loss coefficient $L_3 = 9\Lambda_{\text{ad}}(6\pi/k_T^2)^{3/2} e^{-E_r/(k_B T)}$. L_3 only depends on Λ_{ad} and not on Γ_r evidencing that the

atom-dimer collision process is the limiting effect in the loss.

We now investigate the temperature evolution during the loss process in the thermalized regime and show that either heating or cooling can occur. For simplicity we assume a cloud trapped in a uniform box potential of volume V . We further assume that the thermalization is instantaneous compared to the loss events, as justified by the inequality (A). We first consider a single cascaded loss event where the atoms 1 and 2 form a dimer before colliding with atom 3. We denote as \vec{v}_i the velocity of atom i . Given the assumption of the interacting non-unitary regime, \vec{v}_1 and \vec{v}_2 satisfy $\frac{m}{4}|\vec{v}_1 - \vec{v}_2|^2 = E_r$. Assuming a temperature T of the gas before the collision, the ensemble-averaged (denoted $\langle \cdot \rangle$) values satisfy $\frac{m}{4}\langle |\vec{v}_1 + \vec{v}_2|^2 \rangle = \frac{m}{2}\langle |\vec{v}_3|^2 \rangle = 3k_B T/2$. Therefore the average total energy lost when the three atoms leave the cloud is $\langle E_{\text{loss}} \rangle = \sum_{i=1}^3 \frac{m}{2}\langle |\vec{v}_i|^2 \rangle = E_r + 3k_B T$. In turn, the change in temperature in the gas induced by a single loss event δT_{loss} is deduced from the average energy lost and the average kinetic energy of the three atoms via $\frac{3}{2}Nk_B\delta T_{\text{loss}} = \frac{9}{2}k_B T - \langle E_{\text{loss}} \rangle = \frac{3}{2}k_B T - E_r$ with N the number of atoms in the gas after the loss. As in a box trap $n = N/V$, the rate of total loss events is given by $L_3 n^2 N/3$. This results in:

$$\frac{dT}{dt} = L_3 n^2 \frac{2T}{9} \left(\frac{3}{2} - \eta \right) \quad (7)$$

with $\eta = E_r/k_B T$ called the truncation parameter. Depending on the value of η , the temperature variations are found to change sign. For a small dimer energy such that $\eta < 3/2$, low energetic particles are preferentially lost, resulting in an overall heating of the gas. In contrast, for a large dimer energy such that $\eta > 3/2$, high energy particles are preferentially lost and a cooling of the gas prevails. For a dimer energy such that $\eta = 3/2$, the temperature of the gas is constant because the average kinetic energy of an atom lost is $3/2 k_B T$. Note that the regime $\eta < 3/2$ actually matches the unitary regime (see Section II) and in the interacting non-unitary regime of interest $\eta > 3/2$ and loss-induced cooling prevails.

We now study the evolution with time t of a gas whose initial parameters are defined as $\eta_0 = E_r/k_B T_0$, $T_0 = T(t=0)$, and $n_0 = n(t=0)$. To formulate the time unitless, we use the initial characteristic loss time $\tau = 1/(L_3(t=0)n_0^2)$ (typical time for $N/3$ loss events). FIG. 2 shows the time evolution of the temperature following Eq. (7) as a function of η_0 . As anticipated above, for $\eta_0 = 3/2$, the temperature of the gas is constant. For $\eta_0 < 3/2$, the temperature increases, with an overall change over τ of $T(\tau)/T_0 = 1.12$ for $\eta_0 = 1/2$, and for $\eta_0 > 3/2$, the temperature decreases, with $T(\tau)/T_0$ reaching 0.74 for $\eta_0 = 9/2$. The speed of the temperature change saturates for $\eta_0 > 11/2$, limiting a possible cooling scheme on the characteristic loss timescale. This is because the fast temperature decrease

slows down further losses.

Considering the change in density (Eq. (6)) and temperature (Eq. (7)), the change in phase-space density, $\rho = n(2\pi\hbar)^3/\sqrt{2\pi m k_B T}^3$, is given by [22, 25]:

$$\frac{d\rho}{dt} = L_3 n^2 \frac{\rho}{3} \left(\eta - \frac{9}{2} \right) \quad (8)$$

Here, the time derivative of the phase-space density is found to change sign at $\eta = 9/2$. For $\eta < 9/2$ ($\eta > 9/2$), ρ decreases (increases) with time. The energy-dependent cascaded loss close to p -wave Feshbach resonances can therefore be an eligible method of collisional cooling. Analogous to evaporative cooling, one can use larger dimer energies for higher efficiencies. The evaporation efficiency $\gamma = -\log(\rho/\rho_0)/\log(N/N_0)$ is here given by $\gamma = \eta/3 - 3/2$ [28].

We note that the simple scaling laws extracted above hold for a uniform gas. In presence of a harmonic trap, the density is inhomogeneous and a spatial dependence of the loss behavior is expected. In the case of energy-independent three-body recombination, this is known to yield a so-called "anti-evaporation" effect, i.e. loss-induced heating [29]. We foresee that a spatially dependent loss behavior may temper the cascade-induced collisional cooling discussed above.

B. Non-Thermalized Regime

In the following, we consider the opposite extreme case of $\Gamma_r \ll n\Lambda_{\text{ad}}$, i.e. the break-up of the weakly-bound dimers is negligible compared to the loss process. The relaxation into the deeply-bound dimer is instantaneous subsequent to the dimer creation. This leads to a large inelastic to elastic collision ratio, and therefore a non-thermalized, out-of-equilibrium sample. In this regime, Eq. (5) simplifies to

$$\frac{dn}{dt} = -L_2 n^2 \quad (9)$$

where the inelastic scattering process only depends on Γ_r , with $L_2 = 9\Gamma_r (6\pi/k_T^2)^{3/2} e^{-E_r/(k_B T)}$. This shows a qualitative change in loss behavior from an n^3 dependence in the thermalized regime to an n^2 dependence in the non-thermalized regime. This change is due to the losses being limited by the number of dimers instead of the number of dimer-atom pairs.

Due to the absence of thermalization, the reshaping of the kinetic energy distribution from an initially thermalized sample is determined by the energy-dependent losses. The change in the kinetic energy distribution is described by a differential equation obtained via the extension of Eq. (2) into a velocity dependent description (see appendix B). FIG. 3 shows the change of the kinetic energy distribution for $\eta_0 = 4$. The time is expressed in

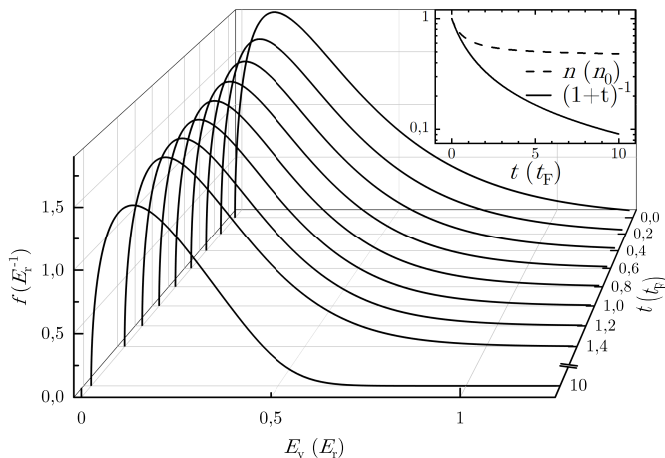


FIG. 3. The kinetic energy distribution $f(E_v)$ of a gas in the non-thermalized regime in units of E_r^{-1} for a truncation parameter $\eta_0 = 4$ after a hold time t in units of t_F in a box potential. Initially, f is a normalized Maxwell-Boltzmann distribution of temperature $E_r/(4k_B)$ and the three-body losses lead to a decrease and reshaping of the kinetic energy distribution. After the axis break, at $t = 10t_F$, the distribution has no more exponential tail of energies $E_v > E_r/2$. The inset shows the density in units of the initial density changing due to a decrease of the kinetic energy distribution (dashed line) and the projected n^2 dependent loss for a gas of constant kinetic energy distribution (solid line). The two curves overlap at times $t < t_F$ and diverge for $t > t_F$ because the depletion of the atoms of high kinetic energies slows down the loss.

units of the characteristic timescale of the losses defined by Eq. (9), $t_F = 1/(L_2(t=0)n_0)$ (analogous to τ). At short times, the change in the energy distribution is dominated by a decrease in amplitude which evidences the atom loss. At later time, we observe a reshaping of the exponential tail at high energy. In particular the kinetic energies $E_v > E_r/2$ are depleted. Finally, the loss stops after this energy tail is fully depleted, as then, no collision process bears enough relative energy to form a weakly-bound dimer. The result is a stable out-of-equilibrium kinetic energy distribution, with a depleted high-energy tail, and without thermalization and no loss. Note that, at this point, other processes that have been neglected such as direct three-body recombination may still contribute.

IV. CONCLUSION

In this work, we extended the previously studied cascade model for a single-component Fermi gas near a p -wave Feshbach resonance in the interacting, non-unitary

regime to combine the description of thermalization and three-body loss. We extract simple scaling laws for the time evolution of the atom number and the temperature in the thermalized case and predict anomalous loss behavior in the non-thermalized scenario. In the latter case, the atom number loss exhibits a n^2 dependence and a yet unexplored behavior of the sample's energy distribution: it is reshaped due to the loss with a particular depletion in the high-energy tail ($E \gtrsim E_r/2$). Within the approximation of our model, the loss vanishes once the tail is fully depleted, leaving a low-energetic, non-thermal steady state. In the opposite regime, i.e. the thermalized case, we find that, in the interacting non-unitary regime ($E_r/(k_B T) > 3/2$), the sample is collisionally cooled at a rate proportional to n^2 . This allows for an increase in phase-space density that can be controlled via the bound-state energy E_r , that is to say, in experiments via the magnetic-field value.

It is interesting to note that cooling or energy removal via three-body loss generally occurs on different timescales as compared to standard evaporative cooling. Furthermore, these timescales can be reduced below typical two-body evaporation timescales at low temperatures by tuning E_r . In the thermalized regime, this could allow for efficient cooling of single component Fermi gases similar to standard evaporation of s -wave interacting fermions. The cooling efficiency is found to be given by $\gamma = \eta/3 - 3/2$, which can be tuned to comparable values as that of standard evaporative cooling $\gamma' \gtrsim 2\eta'/3 - 1$ [30] without relying on s -wave collisions or changing the external trapping potential. Here η' is the standard truncation parameter, i.e. the ratio of trap depth to mean thermal energy, and is typically less than 10 [30]. Finally, we find that the interacting, non-unitary regime in terms of temperature and magnetic detuning from the Feshbach resonance is experimentally accessible using ^6Li , see appendix A. Thus, our findings can be investigated experimentally in future three-body loss investigations of non-unitary p -wave interactions.

ACKNOWLEDGMENTS

We wish to thank Selim Jochim, Hans-Werner Hammer, Binh Tran, Tobias Krom and Robert Freund for fruitful discussions and helpful comments. We are also grateful to Takashi Mukaiyama and Muhammad Waseem for providing the measurement data depicted in FIG 4. This work is supported by the Deutsche Forschungsgemeinschaft (DFG, German Research Foundation) - Project-ID 273811115 - SFB 1225 ISOQUANT and by DFG under Germany's Excellence Strategy EXC-2181/1 - 390900948 (Heidelberg STRUCTURES Excellence Cluster).

- 80, 885 (2008).
- [3] D. S. Petrov, Phys. Rev. A **67**, 010703 (2003).
- [4] D. S. Petrov, C. Salomon, and G. V. Shlyapnikov, Phys. Rev. Lett. **93**, 090404 (2004).
- [5] M. Bartenstein, A. Altmeyer, S. Riedl, S. Jochim, C. Chin, J. H. Denschlag, and R. Grimm, Phys. Rev. Lett. **92**, 120401 (2004).
- [6] T. Bourdel, L. Khaykovich, J. Cubizolles, J. Zhang, F. Chevy, M. Teichmann, L. Tarruell, S. J. J. M. F. Kokkelmans, and C. Salomon, Phys. Rev. Lett. **93**, 050401 (2004).
- [7] M. Bartenstein, A. Altmeyer, S. Riedl, S. Jochim, C. Chin, J. H. Denschlag, and R. Grimm, Phys. Rev. Lett. **92**, 203201 (2004).
- [8] G. B. Partridge, K. E. Strecker, R. I. Kamar, M. W. Jack, and R. G. Hulet, Phys. Rev. Lett. **95**, 020404 (2005).
- [9] C. A. Regal, C. Ticknor, J. L. Bohn, and D. S. Jin, Phys. Rev. Lett. **90**, 053201 (2003).
- [10] J. Zhang, E. G. M. van Kempen, T. Bourdel, L. Khaykovich, J. Cubizolles, F. Chevy, M. Teichmann, L. Tarruell, S. J. J. M. F. Kokkelmans, and C. Salomon, Phys. Rev. A **70**, 030702 (2004).
- [11] V. Gurarie, L. Radzihovsky, and A. V. Andreev, Phys. Rev. Lett. **94**, 230403 (2005).
- [12] C.-H. Cheng and S.-K. Yip, Phys. Rev. Lett. **95**, 070404 (2005).
- [13] F. Chevy, E. G. M. van Kempen, T. Bourdel, J. Zhang, L. Khaykovich, M. Teichmann, L. Tarruell, S. J. J. M. F. Kokkelmans, and C. Salomon, Phys. Rev. A **71**, 062710 (2005).
- [14] T. Nakasuji, J. Yoshida, and T. Mukaiyama, Phys. Rev. A **88**, 012710 (2013).
- [15] J. Yoshida, T. Saito, M. Waseem, K. Hattori, and T. Mukaiyama, Phys. Rev. Lett. **120**, 133401 (2018).
- [16] M. Waseem, J. Yoshida, T. Saito, and T. Mukaiyama, Phys. Rev. A **98**, 020702 (2018).
- [17] M. Waseem, T. Saito, J. Yoshida, and T. Mukaiyama, Phys. Rev. A **96**, 062704 (2017).
- [18] H. Suno, B. D. Esry, and C. H. Greene, Phys. Rev. Lett. **90**, 053202 (2003).
- [19] M. Waseem, J. Yoshida, T. Saito, and T. Mukaiyama, Phys. Rev. A **99**, 052704 (2019).
- [20] J. Li, J. Liu, L. Luo, and B. Gao, Phys. Rev. Lett. **120**, 193402 (2018).
- [21] L. Mathey, E. Tiesinga, P. S. Julienne, and C. W. Clark, Phys. Rev. A **80**, 030702 (2009).
- [22] M. Nuske, E. Tiesinga, and L. Mathey, Phys. Rev. A **91**, 043626 (2015).
- [23] R. Mathew and E. Tiesinga, Phys. Rev. A **87**, 053608 (2013).
- [24] E. Tiesinga, M. Horvath, R. Thomas, A. Deb, and N. Kjaergaard, Nature Communications **8**, 452 (2017).
- [25] S. Peng, H. Liu, J. Li, and L. Luo, “Cooling a fermi gas with three-body recombination near a narrow feshbach resonance,” (2021), arXiv:2107.07078.
- [26] D. V. Kurlov and G. V. Shlyapnikov, Phys. Rev. A **95**, 032710 (2017).
- [27] V. Gurarie and L. Radzihovsky, Annals of Physics **322**, 2 (2007).
- [28] F. Ç. Top, Y. Margalit, and W. Ketterle, Phys. Rev. A **104**, 043311 (2021).
- [29] T. Weber, J. Herbig, M. Mark, H.-C. Nägerl, and R. Grimm, Phys. Rev. Lett. **91**, 123201 (2003).
- [30] W. Ketterle and N. J. van Druten, Advances In Atomic, Molecular, and Optical Physics, **37**, 181 (1996).
- [31] In [19] the notation is K_{ad} for the vibrational quenching rate coefficient.
- [32] J. Fuchs, C. Ticknor, P. Dyke, G. Veeravalli, E. Kuhnle, W. Rowlands, P. Hannaford, and C. J. Vale, Phys. Rev. A **77**, 053616 (2008).
- [33] Due to a difference in the definition of L_3 as compared to [19], our Λ_{ad} is not comparable to their parameter K_{ad} .

Appendix A: Benchmarking of the Cascade Model

To verify our model we compare it to experimental data from Waseem *et al.* [19]. In their experiment they investigate three-body losses of ^6Li in the $|F, m_F\rangle = |1/2, 1/2\rangle$ state close to the Feshbach resonance at 160G for different magnetically tuned positive binding energies E_r on the order of the kinetic energy of the atoms $3/2k_B T$. They extract the three body loss parameter L_3 from a fit of the atom-loss curves (see Eq. (6)). Then they use the cascade model to fit the rate coefficient of the vibrational quenching Λ_{ad} from L_3 [31].

Here we use the L_3 values fitted to their atom-loss measurements and extract Λ_{ad} using the model described in this paper. FIG. 4 shows L_3 for three sets of measurements of thermalized samples at temperature of 2.7 μK , 3.9 μK and 5.7 μK for magnetic field detunings between 150mG and 600mG. The mean densities for the data sets are $n_1 = 1.2 \times 10^{18}\text{m}^{-3}$, $n_2 = 1.3 \times 10^{18}\text{m}^{-3}$, and $n_3 = 1.5 \times 10^{18}\text{m}^{-3}$ for the respective temperatures.

For these measurements, the gas was neither fully in the thermalized nor in the non-thermalized regime with regards to the elastic to inelastic collision ratio, and thus the loss coefficient should be extracted from Eq. (5) for small losses:

$$L_3^{\text{int}} = \frac{9\Lambda_{\text{ad}}\Gamma_r}{n_0\Lambda_{\text{ad}} + \Gamma_r} \left(\frac{6\pi}{k_T^2} \right)^{3/2} e^{-E_r/(k_B T)} \quad (\text{A1})$$

The data in FIG. 4 shows a transition from the interacting non-unitary regime to the non-interacting regime, making a second description of the loss necessary to explain the measurements. Because the assumption that virtually all atoms lost have the collision energy E_r does not hold in the non-interacting regime, the molecule creation rate cannot be approximated with a delta function. Instead, in this regime, the losses are described via direct three-body recombination yielding $L_3 \propto V_p^{8/3}$ and no density dependent regimes [18]. We add the two results for L_3 to describe the crossover of the two regimes:

$$L_3 = L_3^{\text{int}} + C \frac{\hbar}{m} k_T^4 V_p^{8/3} \quad (\text{A2})$$

Here $C = 2 \times 10^6$ is dimensionless and quantifies the coupling strength between the closed channel and the deeply bound state [15]. Eq. (A2) describes the three data sets from FIG. 4 in the crossover regime with Λ_{ad}

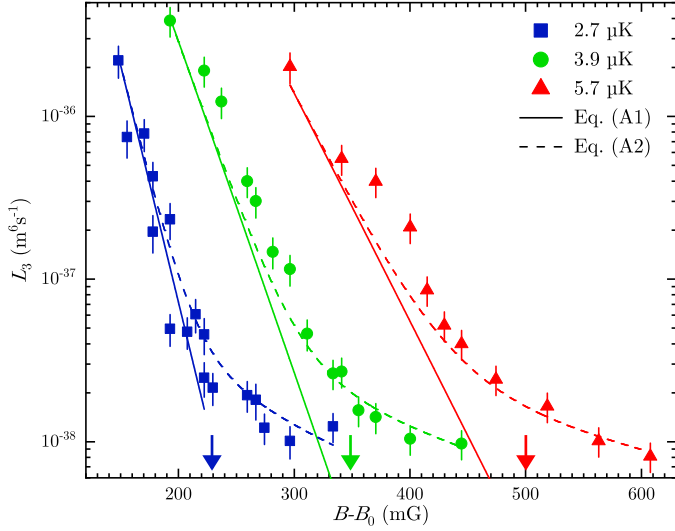


FIG. 4. The three-body loss coefficient L_3 close to the p -wave Feshbach resonance at $B_0 = 159.17(5)$ G from the publication [19] for three different sets of temperatures of 2.7 μ K, 3.9 μ K and 5.7 μ K of squares, circles, and triangles respectively. The arrows mark the point where $E_r/(k_B T_0) = 15$, separating the interacting and non-interacting regime. The dashed curves, describing the crossover between the two regimes, are the result of a fit of Eq. (A2) to the data of the three temperatures with the result of a vibrational quenching rate coefficient $\Lambda_{\text{ad}} = 3.6(6) \times 10^{-14} \text{ m}^3 \text{ s}^{-1}$. The solid curves show the loss coefficient of only the cascade model with the fit result Λ_{ad} included in Eq. (A1).

as only free parameter. We fix the other parameters to the values $E_r = 113 \pm 7 \mu\text{K G}^{-1}$ from Fuchs *et al.* [32] and $k_e = 0.055(5) a_0^{-1}$ from Nakasuji *et al.* [14] and fit Eq. (A2) to the data points.

We weight each data set equally, independent of the number of points. The resulting curves are shown in FIG. 4 (dashed lines), and they are in good agreement with the data. We extract a vibrational quenching rate coefficient $\Lambda_{\text{ad}} = 3.6(6) \times 10^{-14} \text{ m}^3 \text{ s}^{-1}$ [33]. By fitting the data with Eq. (A2) we reduce the relative error to $\Delta\Lambda_{\text{ad}}/\Lambda_{\text{ad}} \approx 0.17$ compared to $\Delta K_{\text{ad}}/K_{\text{ad}} \approx 0.38$ from Waseem *et al.* [19].

It is interesting to note that the bare cascade model of Eq. (A1), using the above extracted Λ_{ad} , explains well the data for each temperature in the regime where the system is close enough to the resonance (solid lines), identifying the interacting non-unitary regime. Comparing Γ_r and $n_0\Lambda_{\text{ad}}$ as extracted above, we get values of

the ratio $\Gamma_r/(n_0\Lambda_{\text{ad}})$ varying between 3 and 24. This indicates that the system can be in a thermalized regime or in a transition regime where elastic and inelastic cascade processes happen at similar rates. We also note that in previous studies with ^6Li [15, 19], $\Gamma_r/(n_0\Lambda_{\text{ad}})$ was varied from 10^{-1} to 10^1 .

Appendix B: Losses in the Non-Thermal Regime

To study the three-body losses in the non-thermalized regime, we extend Eq. (2) into a velocity dependent differential equation in the limit of $\Gamma_r \ll n_0\Lambda_{\text{ad}}$. With the approximation of $K_M(E) \propto \delta(E - E_r)$ for the dimer creation rate, the phase-space density $\rho(\mathbf{v})$ of the atoms changes with every event where a dimer is created and immediately lost via atom-dimer collision. The collision energy of two atoms with velocities \vec{v} and \vec{v}' is $E(\vec{v}, \vec{v}') = m|\vec{v} - \vec{v}'|^2/4$, such that the change in phase-space density is:

$$\begin{aligned} \frac{d\rho(|\vec{v}|)}{dt} = & -2 \int d\vec{v}' K_M(E(\vec{v}, \vec{v}')) \rho(|\vec{v}|) \rho(|\vec{v}'|) \\ & - \frac{\rho(|\vec{v}|)}{n} \int d\vec{v}' d\vec{v}'' K_M(E(\vec{v}', \vec{v}'')) \rho(|\vec{v}'|) \rho(|\vec{v}''|) \end{aligned} \quad (\text{B1})$$

Here the gas is assumed to be trapped in a box potential and $\rho(\mathbf{v}) = n_0 \cdot f(E_v)$ is the product of the initial density of atoms with the kinetic energy distribution. The atom's kinetic energy $E_v = mv^2/2$ is assumed to be independent of the atom's position, and the gas is prepared such that $f(E_v)$ initially is a Maxwell-Boltzmann distribution.

The first part of Eq. (B1) accounts for the process that the atom lost from the distribution with velocity \vec{v} collides with another atom with velocity \vec{v}' to form a weakly bound dimer. In the limit of no thermalization, this dimer is automatically lost from the trap, and thus the loss rate has no additional dependence on the density. The factor of 2 is due to the interchangeability of the two atoms making up the dimer. The second part of the equation accounts for the loss of single atoms due to collision with a dimer, formed beforehand by the collision of two atoms of velocities \vec{v}' and \vec{v}'' . The velocity group of atoms lost this way depends only on the population of the velocity group and the dimer-creation rate. Thus no condition is imposed on the velocity of the atom, and the loss scales with the population of the velocity group.